Presented at: 17th Workshop on Crystalline Silicon Solar Cells & Modules: Materials and Processes, August 5 - 8, 2007, Vail Cascade Resort, Vail, Colorado USA

Fundamental Mechanisms in the Fire-Through Contact Metallization of Si Solar Cells: A Review

Bhushan Sopori,[1] Vishal Mehta,[1] Przemyslaw Rupnowski,[1] Jesse Appel,[1] Manuel Romero,[1] Helio Moutinho,[1] Didier Domine,[1] Bobby To,[1] Robert Reedy,[1] Mowafak Al-Jassim,[1] Aziz Shaikh,[2] Nazarali Merchant,[2] Chandra Khadilkar,[2] Dave Carlson[3] and Murray Bennet[3]

[1] National Renewable Energy Laboratory
[2] Ferro Electronic Materials, Vista, CA
[3] BP Solar, Frederick, MD

ABSTRACT

Metallization-firing of Si solar cells is simple to perform, but it involves a complex synergism of many mechanisms. (1) dissolution of (SiN:H) antireflection coating by the constituents of the Ag ink, followed by Si-Ag interactions at the front contact; (2) diffusion of hydrogen from the interface into the bulk of the cell for impurity and defect passivation; and (3) alloying of the back Al contact to form a back-surface field (BSF). Currently, the firing conditions that yield the best cell efficiency are determined empirically. Such an empirical determination may not represent the highest achievable cell performance. To achieve the highest efficiency, each of these functions must be **maximized**. In addition, the finished contact must also meet other requirements such as mechanical strength, minimum stress, and thermal cycling. We will review the current understanding of contact formation mechanisms and describe the results of our recent work towards developing a coherent understanding of the physics of various mechanisms involved in a fire-through process. We will also present a model for the resistance of a solar cell due to the front contact.

INTRODUCTION

Fire-through metallization is the most common method for forming front-metal contact on a silicon solar cell. In this process, a solar cell is coated with an antireflection film consisting of about 750 Å of SiN:H. A front metallization pattern of Ag-based ink is then screen-printed on top of the SiN:H layer. In many cases, an Al-based contact is also screen printed on the back side of the cell so that both contacts can be co-fired. Next, the cell is fired (≈160secs) in an IR belt furnace in which the cell experiences a temperature profile that peaks typically at about 800°C. This process results in interaction of Ag particles with Si to form an ohmic contact at the front interface. In a co-firing process, an ohmic contact is also formed at the back side due to Al-Si alloying. Furthermore, during this step, H diffuses into the bulk of the cell passivating impurities and defects. Thus, optimization of contact formation involves synergism of three processes:

1. Front contact formation to produce a uniform, low-resistance, ohmic contact with high shunt resistance. Such a contact will produce a high open-circuit voltage (V_{oc}) and high fill factor (FF).

2. Diffusion of H deep inside the material and association of H with impurities and defects to passivate them. Good bulk passivation will yield a high short-circuit current density (Jsc) and high Voc.
3. Formation of Si-Al alloyed region on the backside to produce a large field which can lead to a low surface recombination on the backside with a concomitant high Voc.

A metallization firing influences each of the functions simultaneously. The best cell performance can only be obtained if each of the functions is maximized. However, one can intuitively argue that a process condition that favors maximization of one of the above function may not maximize the other two processes. For example a mild firing may lead to formation of a good front contact but may not diffuse H deep into the bulk. Likewise, a strong firing is required to form a good BSF, but it can cause shunting of the front junction and out diffusion of H. Therefore, it is important to study details of all three of these phenomena and examine how one can select a suitable choice of inks and processes that can maximize the cell performance. One approach to maximizing the cell performance is to tailor the parameters of the SiN:H, front-side ink, and back-contact ink so that each of these functions can be maximized by the same firing cycle, i.e., temperature-time (T-t) profile. This approach requires detailed studies that can separate the mechanisms of each function. This paper will describe the results of our recent work to develop a coherent understanding of the physics of various mechanisms involved in a fire-through process. Because this is ongoing work, we will present results that we have obtained to date. We will also present brief reviews of work published in the literature, which forms the basis of current understanding. Emphasis of this paper is on the front contact formation.

It is important to point out that although the fire-through process is not well understood, it is very successfully used in commercial cell fabrication. As discussed later in this paper, the success of the fire-through process is, in part, due to the formation of the back contact and the diffusion of hydrogen, which have somewhat large process windows and seem to be less sensitive to the process parameters. However, the front contact formation is more critical and difficult to control. This problem is because a good ohmic contact requires Ag to interact with a very shallow layer of Si. In most situations, Ag can locally go deeper toward a junction resulting in the formation of "spikes." Consequently, the FF of solar cells with screen-printed, fire-through contact is typically lower than those formed by photo lithographically that defines a pattern in SiN:H followed by direct deposition of the metallic contact.

MECHANISM(S) OF FRONT CONTACT FORMATION

A good, front contact on a solar cell must have several features, which include: (i) a uniform ohmic contact at the interface typically produced by Si-Ag alloy formation, with a large ratio of Si-Ag/Si area; (ii) a continuous electric contact within the metallization pattern for lateral transport of current with low resistance; and (iii) a minimum coverage of the metal to prevent "shadowing' of the cell by the contact and minimize Si-metal interface.

Silver paste (ink) used for front contact is composed of many ingredients, which undergo a variety of interactions during firing to yield proper electrical, mechanical, and thermal properties. Various ink manufacturers have their proprietary compositions, which can vary to accommodate different requirements. In general, the paste consists of three major constituents: (a) a fine powder of Ag, typically 0.1 to 0.3 μm in size, (b) a glass frit, which can be a mixture of several

glasses containing a host of metal oxides such as lead borosilicate glass, B_2O_3, ZnO, BiO_3,[1-8]and (c) an organic binder[9]. The metal pattern is applied via screen printing which, consists of squeezing the ink through a screen template that has an opening in the form of the metal pattern[10].

The formation mechanism of the fire-through contact that lead to these steps is quite complex and interdependent. There are many hypotheses that speculate on chemical interactions that occur between various constituents of ink during the firing step. While Cheek et al[11] suggested it was liquid phase sintering, Ballif et al[12] have suggested that Si and Ag get dissolved in the glass frit and on cooling the Si recrystallizes and the Ag crystallites grow randomly on silicon. This explanation was based on the observations in over-fired samples. Hillali et al[13] have also suggested dissolution of silver particles in glass layer and subsequent recrystallization of the silver particles upon cooling. This explanation however is counter intuitive because one would expect that under normal firing conditions a significant dissolution of Ag in glass cannot occur. This conclusion was also reached by Schubert et al[14] who performed experiments that indicate it takes a long time for silver particles to get dissolved at normal cell firing temperatures. Schubert et al[15] have suggested that the lead oxide gets reduced by the Si. The generated Pb alloys with the Ag. The Pb-Ag alloys dissolve <100> silicon planes and inverted pyramids get formed. On cooling Ag crystallizes on <111> planes of pyramid. According to Schubert et al, Pb is the transport media of the Ag. Although, we agree with the some part of this model, in our studies, we did not see any pyramids for optimal fired cells.

Young et al[16] have suggested that metal oxide at firing temperatures, in the glass is reduced by Si (i.e. $xSi + 2MO_x = 2M + xSiO_2$). This effect would mean that "solvent metal" (M) is present everywhere glass and Si are in contact. It would also suggest the existence of a thin layer of SiO_2 at the interface. However, a detailed explanation as to what happens in the micro scale is lacking.

Although there are many proposed mechanisms and a great deal of work has been published, a coherent story of the sequence of Si-Ag alloying requires answers to the following questions:
1. What is the actual temperature at which Si-Ag form an alloy and is this alloy formation aided by the presence of M.
2. To what degree does the melting of Ag particles occur?
3. Does Ag get dissolved in glass and re-precipitates as proposed in some references…..?
4. How much Si is consumed in a typical contact formation?

To answer these issues we have performed the experiments as described in the next section, aimed at:
(i) Precise determination of temperature at the Si-metal location during contact formation, so that one can apply information from phase diagrams as a guide to project the degree of melting and composition of the Si-Ag alloy.
(ii) Identification of spatial distribution of various constituents in the ink after firing. This problem arises because interface analysis is typically done by cleaving a fired sample. Because the wafers are typically multicrystalline, the cleavage is typically irregular. Cleavage quality is further degraded by stress in the wafer produced by presence of ink. To overcome this problem, we have developed a cross-sectioning technique. Furthermore, many experiments are done in

unrealistic conditions that may not occur during a typical contact formation. In this paper we describe some results of our studies aimed at identifying the precise temperatures at the Si-metal interface, metal distribution inside the contact using a new cross-sectioning technique that produces highly flat cross-sections.

EXPERIMENTAL PROCEDURE

SiN:H-coated, N+/P cells on single-crystal and multicrystalline (mc)-Si wafers are screen printed with front and back metallization patterns and fired in a static optical furnace —a computer-controlled furnace that applies a predetermined optical flux as a function of time to the cell. We used Ferro's (Ag-based and Al-based) inks of different properties such as composition and particle size, as metallization pastes. The resultant temperature distribution over the cell is measured as a function of time by multiple thermocouples attached to the cells.

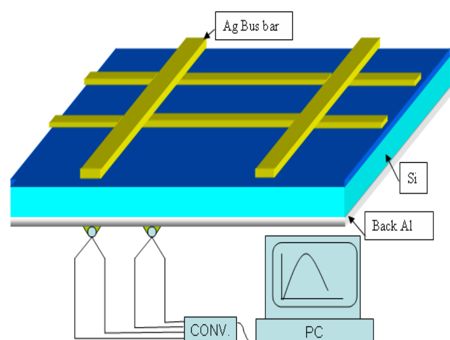

Figure 1. Set up for (T – t) profile. measurement

K-type thermocouples were cement bonded on to the wafers maintaining the same thermal mass (Fig 1). One was directly below the busbar while the other was away from it. The output was measured through special software. Temperature distribution profile of the cell was generated during actual firing.

The fired cells are analyzed by dark and illuminated current-voltage (I-V) measurements to determine cell parameters (V_{oc}, J_{sc}, and FF), series resistance and shunt conductance, and by a variety of analytical techniques including secondary-ion mass spectroscopy (SIMS), Fourier transform infrared (FTIR) spectroscopy, and electron-beam methods.

To perform a detailed statistically meaningful characterization of Si-metal interactions, we have developed a new procedure for cross-sectioning large-area solar cell samples using chemical-mechanical polishing (CMP). This polishing technique generates a large, planar cross-section of the composite (stratified) device that can be analyzed by atomic force microscopy (AFM), conductive AFM (C-AFM), scanning Kelvin probe microscopy (SKPM), and other electron-beam techniques to measure penetration and distribution of metal into Si, and electric potential and field distributions at the Si-Ag and Si-Al interfaces. Because this cross-sectioning technique produces a highly planar surface, it provides access to various components in a segregated composition (such as glass, Ag, Si-Ag alloy in a contact). In comparison, a fractured cross-section (particularly of a mc-Si sample) has artifacts that can interfere with a good image quality.

Fig.2a is an image of the Si-Al interface of a cross-sectioned cell showing a planar view of Al grains in a glass matrix. Fig. 2b is a similar image of the Si-Ag interface (having a much finer particle size of Ag). It is important to point out that a standard procedure of wafer cleavage or breakage produces fracture lines and non-planar regions of different layers that are difficult to image with such clarity.

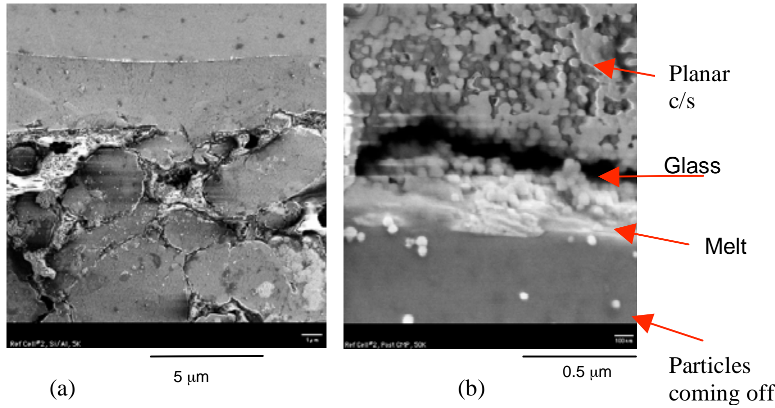

Figure 2. SEM images of a cross-sectioned, fired cell showing: (a) Al back-contact, and (b) Ag front-contact.

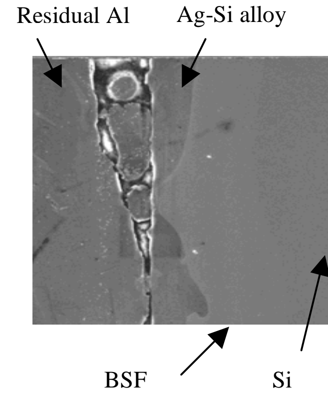

Figure 3. Formation of Al-alloyed regions and the BSF.

Fig.3 shows the Al-Si interface of a cross-sectioned cell in which the unmelted Al was etched away; one can see the Al grains, Si-Al alloy, as well as the BSF. We have studied the formation of BSF and Al alloyed regions for a host of T-t profiles. We found that such regions are nonuniform, but they can produce wide BSF regions.

These analyses are used to measure the following: (1) Distribution of Ag penetration into Si (N+/P), change in the particle size of Ag upon firing, and distribution of solvent metal(s) in the glass matrix, and electric potential and field as a function of depth from the Ag-Si interface. These parameters and the temperature profiles at the metal allow us to establish the chemistry of Ag contact formation; (2) Changes in the H distribution in the SiN:H and near the Si surface; and (3) Dissolution rate of SiN:H in glass, penetration of Ag and Al in Si. Each of these mechanisms is also modeled theoretically to get further insight into the physics of the process.

RESULTS AND DISCUSSION

The above characterization techniques have led to some salient results, described below as examples.

***1. Temperature distribution of a cell during firing*: ** Screen-printed cells can exhibit a large difference in temperature between regions with and without front metallization. Fig. 4 shows the cell temperature profiles directly under the front metal, and away from it, during a typical fire-through process. The optical flux density profile is also shown. From Fig. 4, it can be seen that the maximum temperature reached under the metal is less than 800°C. This has significant importance in identifying interactions between Si and Ag. This temperature is much below the eutectic point of Ag-Si (835°C)[17-19] and melting point of Ag (961.9°C).

The time duration at higher temperatures was only a few seconds. It is believed that there can be no net migration of Ag particles within the finger or busbar in such a short amount of time. There is increase in the particle size because the adjoining particles fuse together. This can only be explained by invoking mechanisms that can depress the eutectic melting point of Ag-Si, such as the presence of other metals and interface energy. It also suggests a need for carefully designed temperature measurements during solar cell processing.

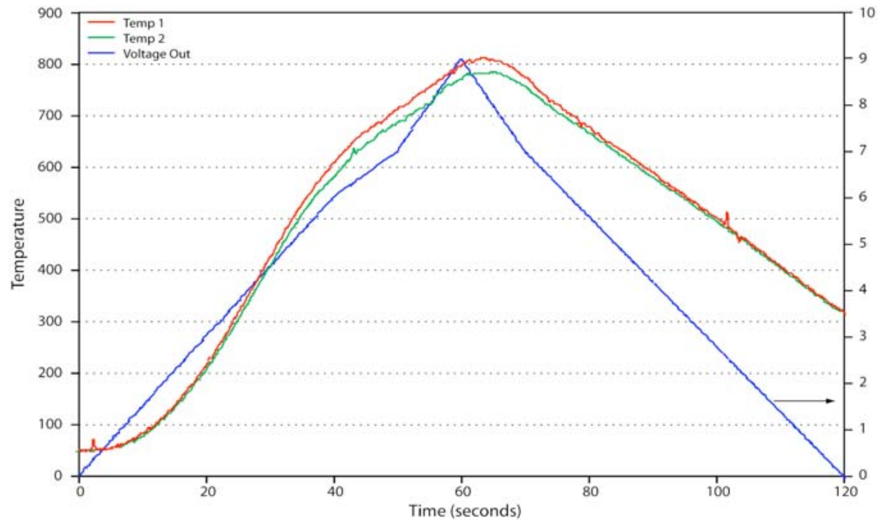

Figure 4. Measured temperature profiles (in °C) under a busbar (green) and away from it (red) during a fire-though process corresponding to the input optical flux (blue).

A direct implication of lower temperature under the front metallization manifests itself in the difference in the hydrogen profile under and away from the metal busbar (see Fig. 5). It is seen that H diffuses deeper in the regions away from the metallization. Because metallization alloys at the surface of N+ region, it can consume the heavily doped surface (see Fig. 6). These results show that significant consumption of P occurs during the Si-Ag interaction, and hydrogen

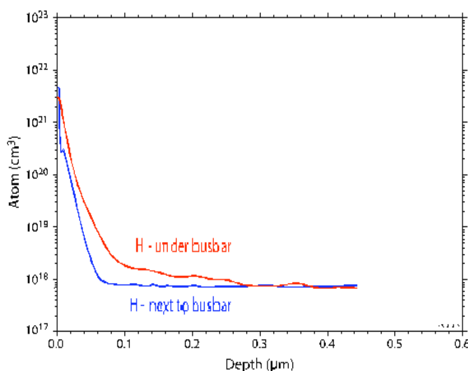

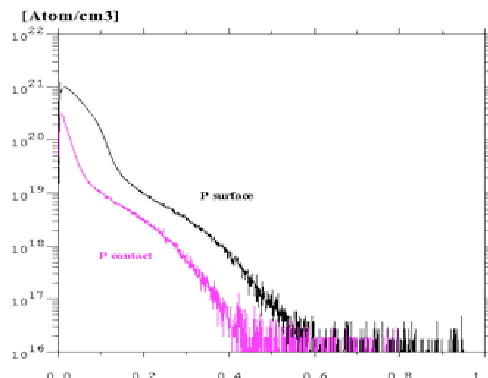

Figure 5. SIMS profiles of H under the metal busbar and away from it. Metal was etched before SIMS analysis.

Figure 6. SIMS profiles of P profiles under the metal busbar and away from it, showing consumption of P by the metal

diffusion is retarded under the metal (creating a lower voltage directly under the metal).

2. Potential, field, and current distributions at the Si-Ag interface. A cross-sectioned cell lends itself to measurements by scanning large-area AFM, SKPM, and C-AFM, without destroying the probe tips. The results provide information on the grain size of the metal, quality of the Si-Ag contact, and structure of the alloyed interface. Fig. 7 shows SKPM measurements at a Si-Ag alloyed region (potential and field profiles are along the white line in the topographic image). Fig. 8 shows a C-AFM image identifying glass phases as insulating regions of low current. Analyses of such images for different T-t profiles show that under optimum alloying conditions, a dense Si-Ag alloy is formed at the interface.

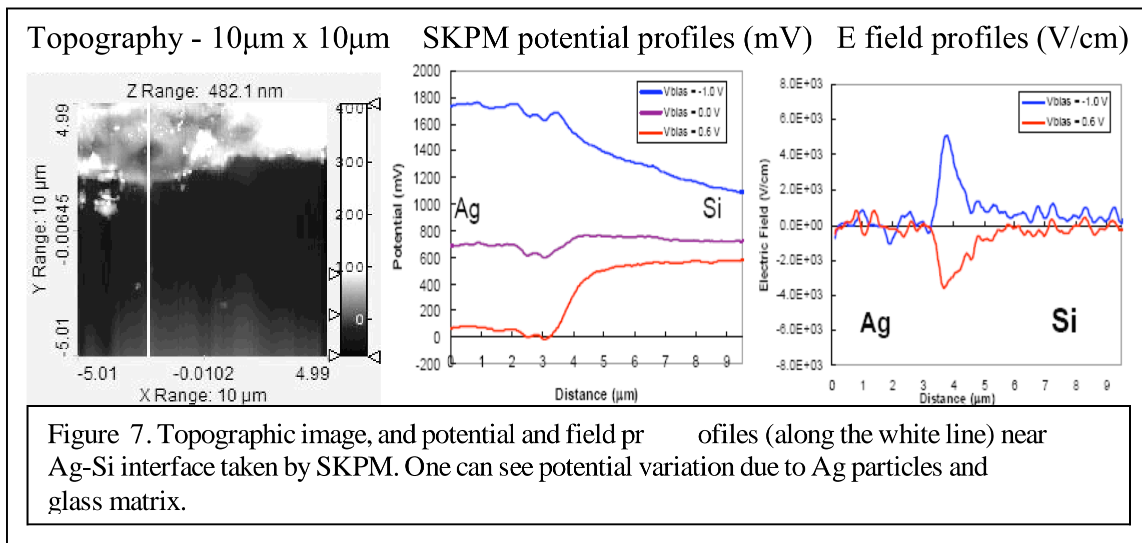

Figure 7. Topographic image, and potential and field profiles (along the white line) near Ag-Si interface taken by SKPM. One can see potential variation due to Ag particles and glass matrix.

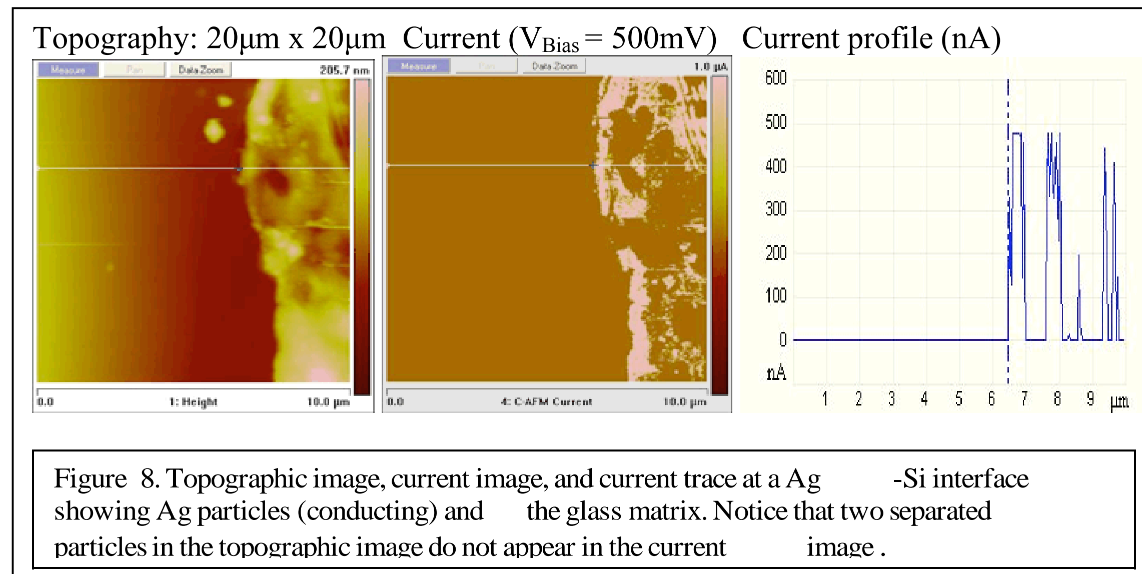

Figure 8. Topographic image, current image, and current trace at a Ag-Si interface showing Ag particles (conducting) and the glass matrix. Notice that two separated particles in the topographic image do not appear in the current image.

3. Dynamics of H diffusion: Our experiments show that there is bilateral flow of hydrogen from SiN:H into Si and into air. This flow is mediated by the damaged layer (and the H trapped in this layer). Because diffusivity of H at the firing temperatures is very large, we expect that extended

firing (i.e., higher temperatures and/or longer times) can result in depletion of H from the bulk of the cell (due to evolution into air and possibly from the backside). It is important to determine the role of the Al back-contact, which can confine H within the cell. Such confinement may occur because of a physical barrier and because of the BSF, which can either aid or retard H ions. These results can play an important role in passivation kinetics and may account for differences in the cell performance between co-fired and separately fired contacts.

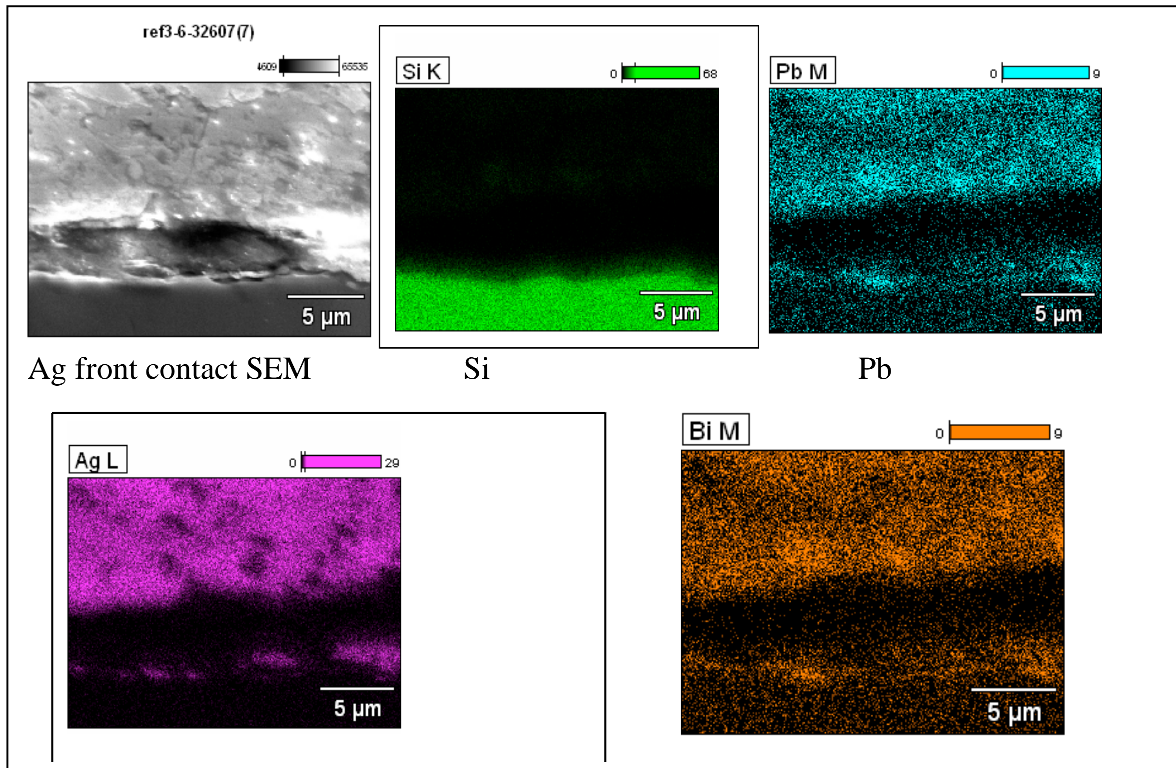

Figure 9. CAFM images of a portion of a silver front contact. Photos mapping various elements i.e., Si, Pb, Ag and Bi are presented

Fig.9 above shows photos of the presence and distribution of various constituent elements in the front contact of a standard solar cell. A big eye-shaped cavity is observed at the Ag-Si interface. We believe this is a void created by the burn-off of a volatile organic vehicle. Based on the T-t profile and the SEM images of the cross-sectioning, we have come up with the contact formation mechanism that is explained in the diagram below (Fig.10).

The contact formation involves a series of interactions between the ink, nitride, and Si. It is generally accepted that in the initial stage of heating (up to 400°C), the frit softens[20] and the softened glass dissolves the SiN:H layer under the paste. Furthermore, molten glass allows some exchange of metal across the boundary of Ag and glass. In particular, M can migrate toward Ag, forming a thin liquid around the particles. As the temperature is increased, many Ag particles agglomerate and fuse together into bunches. At the peak temperature, some of the agglomerates close to the surface react with Si to form a thin alloy layer between Ag particles and Si[21]. It may be pointed out that the alloy formation is not continuous over the Si surface, as shown in the next section. The composition of this molten alloy depends on many factors such as the composition

of the glass frit (particularly metal ions) and the highest temperature during firing etc. The thickness of the layer depends on factors such as temperature, time, and the concentration of P at the Si surface (sheet rho of the N+ layer at the surface). The third stage of the process involves the cool-down. During this stage the molten constituents solidify. As the Si-Ag-M alloy solidifies, it is likely to produce a grading in the composition of interface between Si and Ag[14].

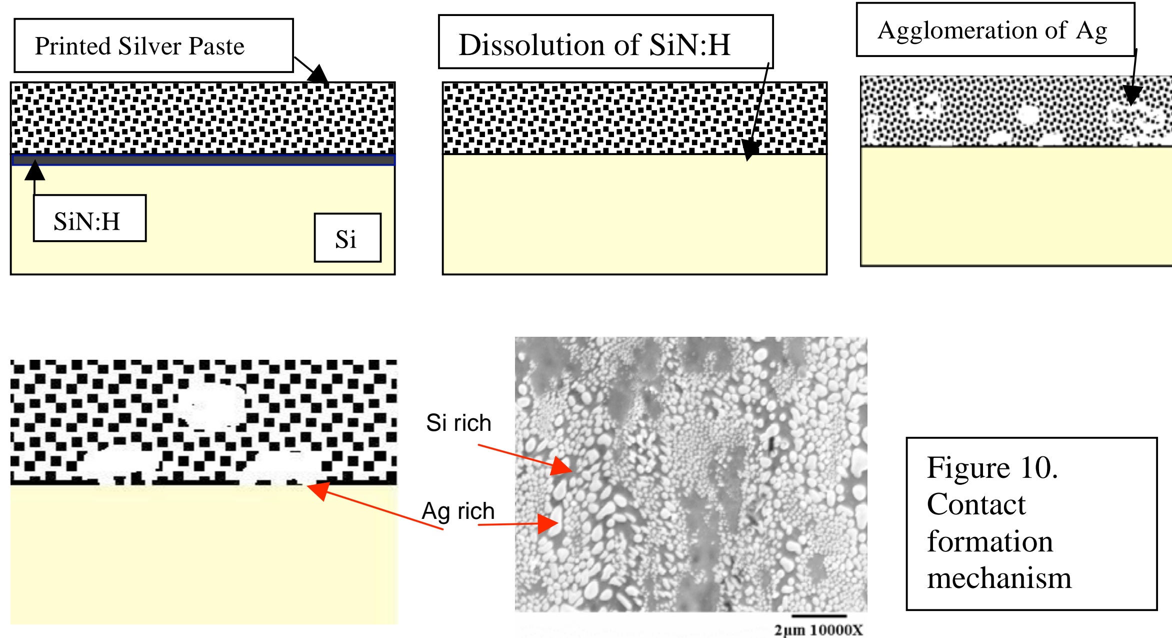

Figure 10. Contact formation mechanism

The top part of the Fig. 10 is a schematic of the Ag finger containing Ag particles and glass frit. The bottom part is the SEM image of the area below the finger or busbar after the Ag finger or busbar has been etched away. In this figure the Ag rich and Si rich area can be clearly seen. The top part explains the possible contact formation mechanism as well as the current transport mechanism. Parallel ohmic, schottky, & tunneling contacts are formed. The amount of each will strongly depend on the contact formation mechanism. As firing temperature increases, there is increase in the particle size because the adjoining particles fuse together. It can be seen that Ag-Si interactions lead to the formation of Ag-rich and Si-rich phases. Formation of an Ag-rich phase depends on many factors, including size of the Ag particles, process conditions, and ink composition. Because the regions of an Ag-rich phase form ohmic contacts at the Si interface, it is desirable to have a large fraction of an Ag-rich phase to produce a cell with a high FF. These results show that the current transport at the front Si interface has two components: a direct Si-Ag ohmic component, and a Si-glass-Ag tunneling component.

CONCLUSION

Some of the important results obtained are: (i) Screen printed cells can exhibit a large (~ 30°C) difference in temperature between regions with and without front metallization. Typically, the maximum temperature reached under the metal is less than 800°C, which is much lower than below the eutectic point of Ag-Si. (ii) A direct implication of lower temperature under the front metallization results in a lack of hydrogen diffusion directly under the metal busbar. However, significant consumption of phosphorous occurs during Si-Ag interaction. (iii) Ag-Si interactions lead to formation of Ag-rich and Si-rich phases. Because an Ag-rich phase forms an ohmic

contact at the Si interface, it is desirable to have a large fraction of an Ag-rich phase to have a high fill factor of the cell. (iv) Al-alloyed regions are not uniform but can produce wide BSF regions. One approach to maximizing the cell performance is to tailor the parameters of SiN:H, front-side ink, and back-contact ink so that each of these functions can be maximized by the same firing cycle, i.e., temperature-time (T-t) profile.

REFERENCES

1. Chung, Y.S. and Kim, H.G. Effect of Oxide Glass on the Sintering Behavior and Electrical Properties in Ag Thick Films. Ieee Transactions On Components, Hybrids, And Manufacturing Technology 11, 195-199 (1988).

2. Nakajima, T., Kawakami, A., and Tada, A. Ohmic contact of conductive silver paste to silicon solar cells. 580-586.

3. Rane, S.B., Seth, T., Phatak, G., Amalnerkar, D., and Ghatpande, M. Effect of inorganic binders on the properties of silver thick films. Journal of Materials Science: Materials in electronics **15**, 103-106 (2004).

4. Oba, T and Inaba, A. Sintering behavior of silver with various glass frits. Electronic Manufacturing Technology Symposium, 1995, Proceedings of 1995 Japan International, 18th IEEE/CPMT International.

5. Gzowski, O., Murawski, L., and Trzebiatowski, K. The surface conductivity of lead glass. J. Phys. D: Appl. Phys. **15**, 1097-1101 (1982).

6. Thuillier, B, Berger, S, and Boyeaux, J. P Laugier A. Observation of mechanisms of screen printed contact formation during heat treatment on multicrystalline silicon solar cells by transmission electron microscopy. 28th IEEE PVSC 2000
Notes: Pages 411-413

7. Lin, J.C. and Wang, C.Y. Effect of surface properties of silver powder on the sintering of its thick-film conductor. Materials Chemistry and Physics **45**, 253-261 (1996)

8. Sun, T., Miao, J., Lin, R., and Fu, Y. The effect of baking conditions on the effective contact areas of screen-printed silver layer on silicon substrate. Solar Energy Materials & Solar Cells **85**, 73–83 (2005)

9. Yiwei, A., Yunxia, Y., Shuanglong, Y., Lihua, D., and Guorong, C. Preparation of spherical silver particles for solar cell electronic paste with gelatin protection. Materials Chemistry and Physics **104**, 158–161 (2007).

10. S. E. Shaheen, R .Radspinner, N. Peyghambarian, and G.E. Jabboura. Fabrication of bulk heterojunction plastic solar cells by screen printing, Applied Physics Letters **79**, 2996-2998 (2001).

11. Cheek, G., Mertens, R., Overstraeten, R., and Frisson, L. Thick-Film Metallizatiora for Solar Cell Applications. IEEE Transactions On Electron Devices **Ed-31**, 602-609 (1984).

12. Ballif, C., Huljic, D.M., Willeke, G., and Hessler-Wyser, A. Silver thick-film contacts on highly doped n-type silicon emitters: Structural and electronic properties of the interface. Applied Physics Letters **82**, 1878-80 (2003)

13. Hilali, M M, Rohatgi, A, and To, B. A Review and Understanding of Screen-Printed Contacts and Selective–Emitter Formation. 14th Workshop on Crystalline Silicon Solar Cells and Modules. 2004, 1617 Cole Boulevard, Golden, Colorado 80401-3393, National Renewable Energy Laboratory.

14. Schubert, G, Fischer, B, and Fath, P. Formation and Nature of Ag Thick Film Front Contacts on Crystalline Silicon Solar Cells Proceedings of the Photovoltaics in Europe Conference

15. Schubert, G, Huster, F, and Fath, P. Current Transport Mechanism In Printed Ag Thick Film Contacts To An N-Type Emitter Of A Crystalline Silicon Solar Cell. 19th European Photovoltaic Solar Energy Conference,Notes: 813-816

16. Young, R J S and Carroll, A F. Advances in front-side thick film Metallization for Silicon solar cells.16th European Photovoltaic Solar Energy conference. Notes: 1731-1734.

17. Weber, L. Equilibrium solid solubility of silicon in silver. Metallurgical and Materials transaction A **33A**, 1145-1150 (2002).

18. Rollert, F., Stolwijk, N.A., and Mehrer, H. Solubility,diffusion and thermodynamic properties of silver in silicon. J. Phys. D: Appl. Phys. **20**, 1148-1 155 (1987).

19. Olesinski, R., Gokhale, A., and Abbaschian, G. The Ag-Si (Silver-Silicon) System Bulletin of Alloy phase Diagram **10**, 635-640 (1989).

20. Prudenziati, M., Moro, L., Morten, B., Sirotti, F., and Sardi, L. Ag-based thick-film front metallization of silicon solar cells , Active and Passive elec. Comp. **13**, 133-150 (1989).

21. B. Sopori and V.R. Mehta. Contact Formation on Silicon Solar Cells: A Review to be published.